Tribology Letters, Vol. 20, Nos. 3–4, December 2005 (© 2005)
DOI: 10.1007/s11249-005-8551-0

Frictional responses of Octadecyltrichlorosilane (OTS) and 1H, 1H, 2H, 2H-Perfluorooctyltrichlorosilane (FOTS) monolayers self-assembled on aluminium over six orders of contact length scale

O.P. Khatri, D. Devaprakasam and S.K. Biswas*

Department of Mechanical Engineering, Indian Institute of Science, Bangalore 560012, India

Received 10 February 2005; accepted 9 September 2005

We have measured the frictional responses of two silane molecules (Octadecyltrichlorosilane; OTS and 1H, 1H, 2H, 2H-Perfluorooctyltrichlorosilane; FOTS) self-assembled on an aluminium substrate in their non heat-treated and heat-treated states. We varied the contact length scale by performing the experiments in atomic force microscope, nanotribometer and macro scale pin-on-disc machine. We have found that conformational disorder and molecular stiffness have major influences on friction in strongly distinguishing the response of OTS from that of the FOTS molecules. The frictional identity between the two molecules before and after heat treatment, though somewhat contrary to that suggested from purely surface energy considerations, is found to hold over six orders of contact length scales, ten orders of normal load and in three vastly different contact conditions; (a) the probe penetrates about 25% of the molecular backbone of a SAM; no substrate deformation, (b) the contact of the probe with the SAM is conformal and the substrate is plastically deformed and (c) the molecule is dispersed in 5% (v/v) concentration in *n*-hexadecane to lubricate a pin-on-disc contact.

KEY WORDS: friction, self-assembled monolayer, conformational order, molecular stiffness, length scale

1. Introduction

The need to conserve energy has propelled an interest to shift from iron based to light metal based engineering components for power generation and transmission. Tribology of metals such as aluminum and magnesium which may find more extensive use, for example in automotive industries, poses new challenges. One such challenge is in selection of additives which can protect light metal components under boundary lubrication conditions. These metals in their manufactured state are persistently covered with layers of oxides and hydroxides. We have therefore looked for additive molecules with head groups which can reactively anchor on these surfaces. Commercially available organosilane additive are being considered presently [1–6] for lubrication of semiconductor silicon surfaces and components in electronic packaging, micro electro-mechanical system and information storage. We consider these molecules here as possible boundary lubrication additive for aluminium based components in moving machinery. These are organosilanes which adhere to the aluminium substrate through oxygen atoms by chemisorption bonding [7,8]. Given this anchoring of silane molecules to the aluminium substrate the objective will be to optimize the chemistry, structure of the terminal end and the backbone of molecules, for tribology. It is known that the adhesion [9,10] and surface energy [11] of CF_3 terminated molecules are somewhat less than that of a CH_3 terminated molecule although there appears to be some experimental evidence to the contrary [3,4]. Lateral Force microscopy studies [1,2,5] however clearly demonstrated that friction corresponding to the former is significantly higher than that of the latter.

Now it is established that molecular conformation of backbone has a profound effect on tribology [12], higher entropy generation and diminishing packing density [13,14] promotes higher friction. It is argued [10,15] that this encourages additional channels of energy dissipation through the excitation of molecular motion. A number of structural parameters such as size of atoms (fluorine is bigger then hydrogen), chain length [10], lateral polymerizability [16], the crystalline phase [2] and the lattice parameters of the substrate material [17] influence the entropy and density of the molecular assembly. External variables such as temperature [18] and pressure [19, 20,13] influence adhesion and friction similarly, this ability being itself a function of the apriori structure [21]. In a boundary lubrication regime as two mating asperities approach each other, make contact, generate heat and then move away from each other. Energy is dissipated through friction as a molecule adsorbed on the substrate is subject to a thermal cycle. If

*To whom correspondence should be addressed.
E-mail: skbis@mecheng.iisc.ernet.in

the process is irreversible the next contact encounters a disordered assembly. We have concluded [22] on the basis of our studies of alkanethiol chain length that the potential for entropy change due to change in temperature is dependent on the apriori defect density in the molecule. We have extended this approach here to two commercially available molecules; octadecyltrichlorosilane (OTS) [8] and 1H, 1H, 2H, 2H-perfluorooctyltrichlorosilane (FOTS) [7]. These are potentially useful molecules as boundary lubricants for aluminium. For these molecules it has been recorded that the increase in disorder is modest upto a heat treatment peak temperature of 483 K for OTS and 573 K for FOTS. FOTS is thus more thermally stable then OTS in spite of the latter being laterally polymerisable [8]. The OTS and FOTS differ not only by the fact that they are hydrogen and fluorine terminated, respectively but also the backbone in OTS has a zig-zag configuration while that in FOTS has a helical structure.

The objective of this work is to elucidate the mechanism of friction of organic molecules self-assembled on rigid substrates with a perspective to optimize selection or design of molecules for a specific application. Two issues need to be addressed in this regard. The first is the problem of length scale (contact area). Considering that the application of these self-assembled monolayers (SAM) span many orders of length scales the work done so far (reviewed as above) is restricted to nano-scale where only 10–50 molecules are involved in contact. Further considering that conformational disorder has been suggested as one of the main physical mechanism for friction, the frictional data generated has only local relevance and repeated experiments generate a large scatter [1]. Given this, our concern is in our ability to distinguish between the performance of any two molecules or any two treatments the SAM is being subjected to. The corollary to this is to question the validity of the suggested mechanism over a large length scale. A similar ambiguity [23] also exists regarding the role of molecular stiffness in governing friction. We address both these issues here by testing two molecules of similar hydrophobicity in their terminal functionality and situated on the same substrate but with distinct states of apriori conformational disorder introduced by steric hindrance. They also have different backbone structures; this makes a large difference to their measured molecular stiffness. Adhesion and friction independently and in relation to each other are governed by conformational disorder. We deliberately change the conformational order even further by heat-treating the molecules and explore the tribology of test molecules before and after heat treatment over six orders of contact length scale.

To do this we organized a wide range of contact environments and measure friction.

1. In an atomic force microscope where a silicon nitride tip of 50 nm diameter is slid against the test molecules, self-assembled on an aluminium substrate. The tests are done in controlled humidity and in water medium. The mean Hertzian pressure at a load of 8 nN is about 90 MPa and the contact radius is 6.7 nm (10^{-9} m).
2. In a nanotribometer where a 2 mm diameter steel ball is slid against the test molecules self-assembled on aluminium flat substrate in the ambient. The mean Hertzian pressure at a load of 50 mN is about 22 MPa and the contact radius is 33 μm (10^{-6} m).
3. In a macrotribometer where the flat end of a 3 mm diameter steel cylinder is slid against an aluminium disc lubricated with the test molecules dispersed in 5% (v/v) concentration in *n*-hexadecane oil. The mean pressure at a test load of 60 N is 8.5 MPa.

2. Experimental

2.1. Materials and sample preparation

Polycrystalline Aluminium containing 97.25% aluminium, 1% silicon, 0.6% magnesium, 0.5% manganese and 0.35% iron is used as substrate. Octadecyltrichlorosilane and 1H, 1H, 2H, 2H-perfluorooctyltrichlorosilane (Lancaster synthesis, UK) were used as received. Iso-octane (99.5%, dry) and *n*-hexadecane (99 + %, anhydrous) (Sd-fine-chem, India and Sigma-Aldrich, USA, respectively) were used as organic solvent. Deionised water, obtained by processing of distilled water through millipore purification (Milli-Q, USA) system, was used to hydrolyze the substrate. Aluminium samples were polished mechanically (sequentially with a 1–3 μm and a 0.25 μm diamond paste) to obtain 5–8 nm RMS (root mean square) roughness and were then sonicated with acetone for 15 min to remove all polishing debris. The polished samples were kept in air for one hour to generate a natural oxide film on the substrate and were then sonicated with millipore water for 30 min. The substrates were flushed with a stream of dry nitrogen gas and were preserved in a desiccator. Before deposition of SAM, samples were kept in (UV) ultraviolet cleaning chamber (Bioforce nanosciences, US) for 30 min to burn all carbonaceous contaminations, which block the adsorption sites. The aluminium samples prepared as above, were immersed in a freshly prepared additive solution (1 mM) for one hour, taken out, rinsed and washed with isooctane (twice) for 10 min to remove excess and physiadsorbed molecules.

2.2. FTIR analysis

All spectra were taken by infra-red reflection absorption spectroscopy (IRRAS) (GX spectrometer,

Perkin Elmer, USA). The instrument is equipped with a liquid nitrogen cooled mercury cadmium telluride (MCT) detector. All IR spectra reported here are referenced to bare aluminium substrate over 712 optimized scan at $4cm^{-1}$ resolution by using p-polarized beam. The sample and detector chambers were purged with nitrogen gas before starting the experiments and at regular intervals. A heating accessory (Harrick scientific corporation, New York, USA) was used for taking the spectra at different temperatures with an incident angle of 75° from the surface normal. The spectral analysis was carried out using spectrum 3.02 version software (Perkin-Elmer, USA).

2.3. Contact angle measurement and surface free energy

The sessile drop contact angle measurements (θ) of SAMs were performed with millipore water and methylene iodide (Lancaster synthesis, UK) using a goniometer with an autopipetting attachment (Rame Hart 100–00, USA). An approximate estimate of the surface free energy (24) value for SAM modified surfaces is obtained by resolving the surface energies contributed to from the dispersion and dipole hydrogen bonding force components using contact angle of SAM with water and methylene iodide.

2.4. Lateral force measurement

All AFM experiments were performed using an "EXPLORER" (Thermo Microscopes, Santa Barbara, USA) with Si_3N_4 cantilevers (Thermo Microscope, CA, USA) associated with a pyramidal tip of nominal radius of 50 nm. The cantilever normal stiffness was found using thermal vibration technique, built into the software. A *V*-shaped cantilever of stiffness 0.1 N/m was used in all the experiments. All the tips were cleaned in an UV chamber for 20 min before experiments. Pull off force and lateral force measurement were carried out in a 0% relative humidity (custom made air tight humidity chamber was used) as well as in water medium (Millipore water). Ultra pure nitrogen gas, which contains 2 ppm water, was used to purge the humidity chamber and generate 0% relative humidity. The normal sensor response was calibrated by taking force curves slope on freshly cleaved mica. Deflections were recorded as a function of piezo movements during both approach and retraction of the cantilever and all adhesion experiments were performed in a peak load range of 0–20 nN. These were converted into force-separation curves. 250–300 force curves were generated for each experimental condition. An average value and standard deviation of the pull off force obtained from these repeated experimental results are reported here. For lateral force measurements [25], we considered the difference in forces recorded in the forward and reverse scan and we report here an average of this difference. The lateral force was recorded using $1\mu m \times 1\mu m$ scan area at different loads (0–25 nN) with a scan rate of 11 μm/s. The lateral force calibration method is reported elsewhere [25].

2.5. Stiffness Measurement

We used a dual double cantilever based "surface force" type apparatus, designated as contact force apparatus [26–28] to measure stiffness. The equipment consists of two parallel and coaxial dual double cantilever flexures. One of the flexures carries a ruby probe (radius: 1.12 mm) and the other a SAM coated aluminum substrate. We compressed the monolayer and vibrated the pressing probe sinusoidally at sub-resonance frequency of 5 Hz and an amplitude of 0.5 nm to record the dynamic response of the platform. Using a visco-elastic model, the stiffness of the SAM is deconvoluted.

2.6. Nanotribometer

Tribological experiments were carried out in the 25–100 mN load range using a ball on disc tribometer (Nanotribometer, CSM Instruments, Switzerland). The ball used 100 Cr6 steel and has a diameter of 2 mm. The steel ball was cleaned with acetone in an ultrasonic bath prior to the experiment. Two sensing mirrors attached to the cantilever head (which carries the ball at one end), perpendicular to each other (*X* and *Z* axis) measure displacements of the cantilever during sliding. During sliding, the friction coefficient is continuously calculated from measuring the *X* and *Z* displacements of the cantilever. All measurements were carried out under ambient conditions (relative humidity: 42%, temperature: 296 K). The sliding speed was kept at 0.1 cm/s.

2.7. Macrotribometer

Macrotribological tests were carried out on a pin-on-disc machine (DUCOM, Bangalore, India). The flat face of a high speed steel pin of 3 mm diameter, loaded (60 N) normally is pressed against the flat surface of an aluminium disc rotating at a linear speed of 0.2 m/s. Both the disc and the pin surfaces were ground to a roughness of 0.2–0.4 μm CLA (Centre Line Average) range. The frictional force is measured by a load cell (resolution 0.1 N) attached to the pin holder. *n*-Hexadecane was used as base oil and was dispersed with 5% (v/v) of OTS or FOTS. Prior to an experiment a full pin-on-disc contact was established by running in; load 5 N speed 50 rpm. For the lubricated tests, a drop of oil (20 μl) dispersed with the additives was placed at the interface, the normal load was applied and the test was commenced. Each test was conducted for 20 min.

3. Results and discussion

Figure 1 shows the methylene antisymmetric stretch (d^-) frequency shifts, during heat-treatment of the SAM to different peak temperatures obtained from FTIR spectra. We have noted desorption of OTS [8] and FOTS [7] at temperatures above 483 K and 603 K respectively. The peak frequency (d^-) shifts towards higher frequency for OTS indicate that the residual disorder in the molecular backbone after a thermal cycle increases steadily with heat-treatment peak temperature. For FOTS there is no residual disorder after heat-treatment at a temperature of about 423 K. At higher temperatures the residual disorder increases, albeit more gradually in the case of OTS, with peak temperature. Figure 2 shows strong siloxane (–Si–O–Si–) peaks at 1072 and 981 cm^{-1} (antisymmetric and symmetric stretch respectively) for the OTS but for FOTS these peaks are very poor and also shows silanol peak at 892 cm^{-1}. This indicates cross

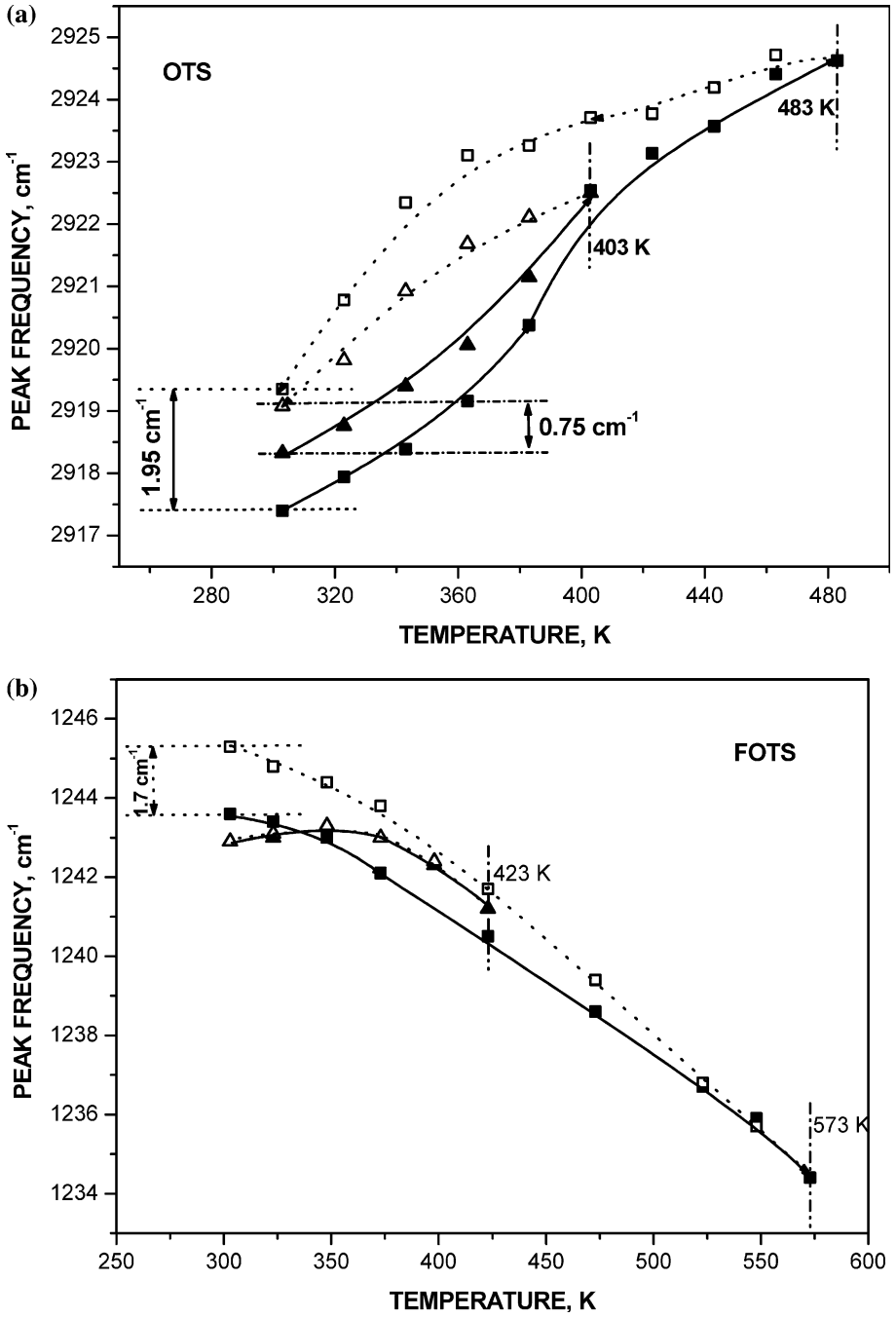

Figure 1. Temperature dependence of peak frequency (IRRAS experiment) for different thermal cycles. (a) CH_2 antisymmetric stretch for OTS SAM on aluminium. Peak temperatures in the cycles are (■) 483 K and (▲) 403 K. Peak frequency shifts are 1.95 cm^{-1} and 0.75 cm^{-1} for $T_{303–483\ K}$ and $T_{303–403\ K}$ cycles. (b) CF_2 antisymmetric stretch for FOTS SAM on aluminium. (■) 573 K and (▲) 423 K. Peak frequency shifts are 1.7 cm^{-1} and 0.0 cm^{-1} for $T_{303–573\ K}$ and $T_{303–423\ K}$ cycles. Filled symbol is for heating and open symbol is for cooling.

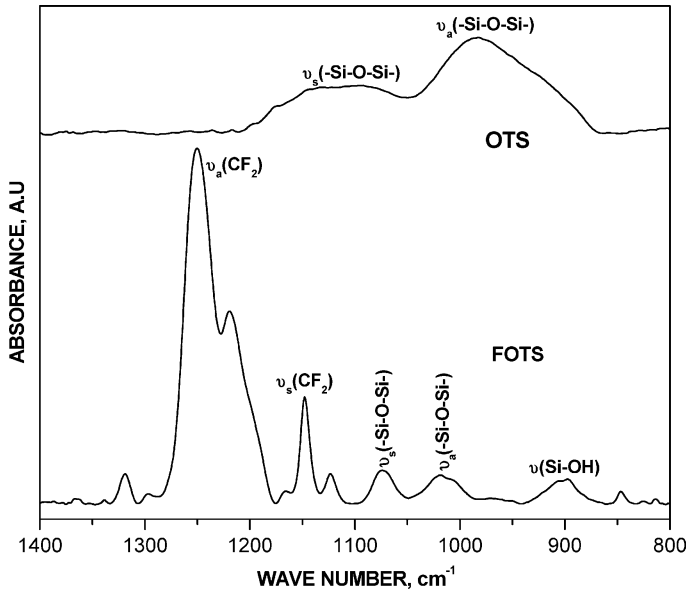

Figure 2. FTIR spectra of OTS and FOTS SAM on aluminium. In OTS spectra two bulk peaks (fused to each other) are due to –Si–O–Si– antisymmetric and symmetric stretch (1072 and 981 cm^{-1} respectively) indicating presence of siloxane network, however in FOTS same peaks are very poor (1074 and 1018 cm^{-1}) as well as there is a presence of Si–OH (892 cm^{-1}) peak indicating low degree of polymerization.

polymerization [8] of silanol group across the surface to result in a two dimensional –Si–O–Si– network for OTS. Cross polymerization provides a constraint in the form of –Si–O–Si– bond length of ≈3 Å [10] which is significantly less than the equilibrium distance of ≈4.7 Å between the two adjacent alkyl chains in monolayer. The steric hindrance imposed by the alkyl chain leads to molecular disorder as reflected by the inability [8] of the molecule to form well ordered crystalline assembly. There is only a low degree of such polymerization in FOTS.

The surface free energy of the test SAMs (figure 3) scales with its conformational order. The FOTS SAM shows lower surface free energy than OTS and the energy increases with increase in heat-treatment peak temperature. The values reported here agree well with those reported by others [9, 11]. Moving now to the lateral force data (nN level of load in the AFM), Figure 4 shows that over the test load range the friction force is linear with finite intercept at zero load. We may represent the characteristics as

$$F = F_s + F_r = F_s + \mu_k L$$

where F_s is the friction force at 0 nN applied load (L) and, μ_k is the coefficient of friction at $L > 0$. As the interactions are highly localized (85–95 molecules are in contact at 8 nN load), there is a large scatter in data which increases dramatically when the molecules become disordered due to heat-treatment. Figure 4 shows that for a molecule there is a coefficient of friction (μ_k) which is constant over the test range of loads, for both the molecules tested before and after heat treatment. Figure 5 shows the area of contact to increase linearly with normal load for FOTS (see Appendix for details of deconvolution of this data from the measurement of contact stiffness (figure 6) using the CFA). This taken with the observation on the coefficient of friction implies an adherence to Amontons law. At 8 nN load if the contact was purely Hertzian the penetration of the tip is about 5–8 Å (taking the SAM modulus as 1–2 GPa) in a SAM which is 1.65 nm long for FOTS and 2.5 nm long for OTS. At this load we can also estimate the elastic deformation of the aluminium substrate to be negligible and that there is no yield in the substrate. The friction force recorded thus pertains to interaction at the terminal end of the SAM only.

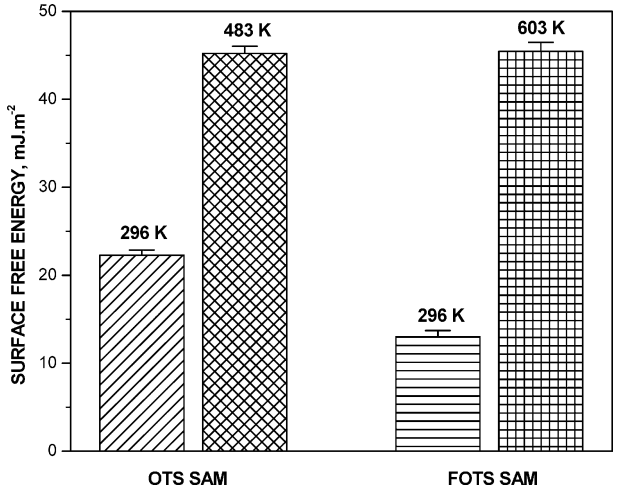

Figure 3. Surface free energy of OTS and FOTS monolayer at 296 K (line bar) and after heat-treatment temperatures 483 K and 603 K for OTS and FOTS respectively (cross net bar), obtained using contact angle measurements. The standard deviation ($+\sigma$) is shown.

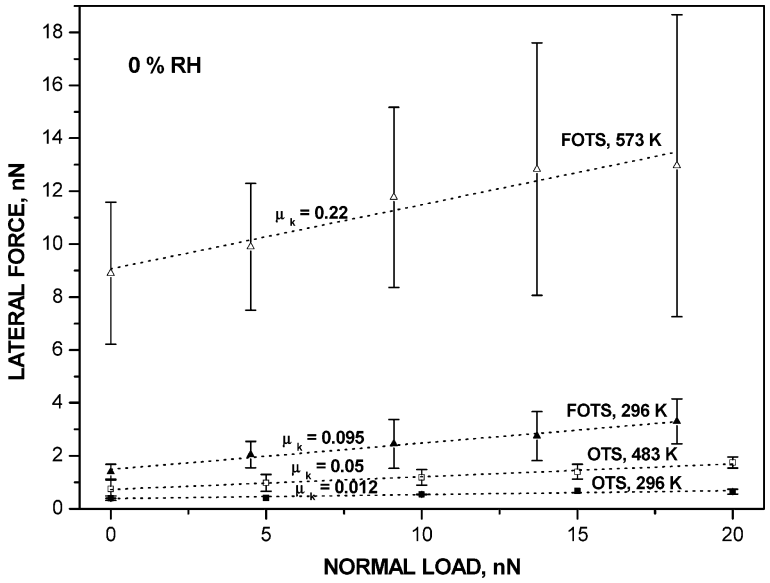

Figure 4. Comparison of lateral force for (■) OTS and (▲) FOTS SAM at temperature 296 K and same open symbols for heat-treatment peak temperatures 483 K and 573 K respectively. Lateral force measurements were carried out at 0% relative humidity at different normal loads. The standard deviation ($\pm\sigma$) is shown.

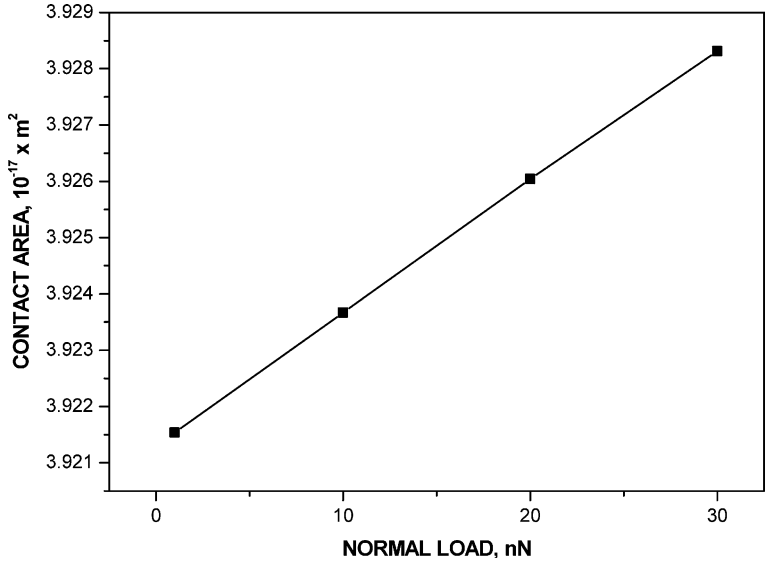

Figure 5. Variation of contact area with applied load, for FOTS on aluminium. The estimation has been done using a Contact Force Apparatus and a 1.12 mm diameter ruby ball of 0.25 RMS (root mean square) roughness (see Appendix for details).

Carpick *et al.* [12] have reviewed other works to indicate that as the surface energy increases, adhesion increases and the friction increases in proportion. Accordingly our surface energy results should yield the following identities in F_s (RT – room temperature, HT – heat-treatment)

$$F_{s(HT)} > F_{s(RT)} \text{ and } F_{s(OTS,RT)} > F_{s(FOTS,RT)}$$

The LFM results in general vindicate the first identity but not the second. The latter, $F_{s(FOTS)} > F_{s(OTS)}$ however corroborates the observations of Kim [23] and Sung [1] at the nN load level. We pursue this result firstly at the low load (nN) level and then at the high load (mN and N) levels. As the surface energy of OTS is greater than FOTS, at 0% humidity $F_{s(FOTS)} > F_{s(OTS)}$ is possible only if OTS is able to generate lubrication while FOTS does not. We must first state that the number "0%" that we cite in describing the humid condition inside the humidity chamber, cannot be considered in absolute terms to describe the conditions at the contact between the tip and the SAM. This number is a record of a hygrometer situated 20 cm away from the AFM inside the chamber. Further the dry nitrogen gas we use to purge the chamber for 20 min at this level of hygrometer reading contains

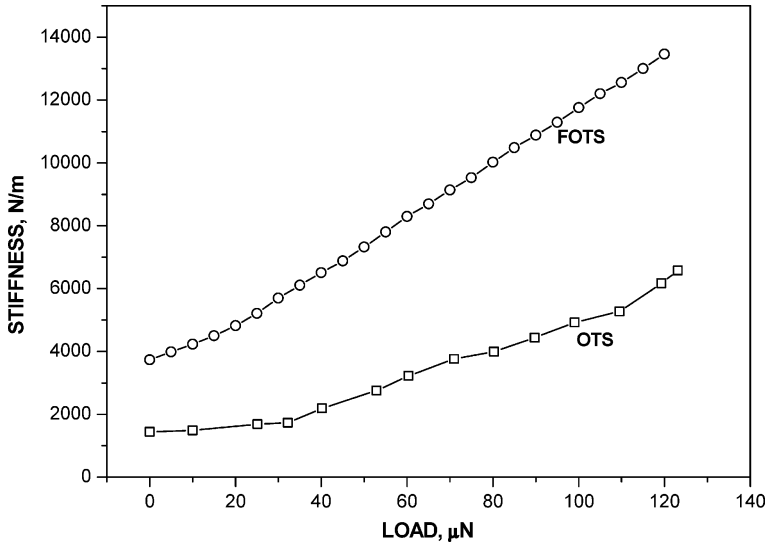

Figure 6. Stiffness of OTS (□) and FOTS (○) SAM on aluminium were measured by Contact Force Apparatus using A/C modulation technique. The measurements were carried out at an excitation of 0.5 nm amplitude and 5 Hz frequency.

about 2 ppm of water (Goyal MG gases, India). The number 0% therefore does not provide information about the possible existence of some adsorbed water molecules on the tip and the SAM surface.

The lowest humidity at which (discounting UHV experiments) friction has been recorded in the past [29–31] is 5%. At 5% humidity where there is insufficient water to form a capillary junction Qian et al. [29] in fact show that hydrophobic/hydrophobic interaction registers a slightly higher friction and a significantly higher adhesion than what is recorded for the hydrophilic/hydrophobic interaction. Assuming that there are fragments of an adsorbed water monolayer present at our 0% humidity contact we use the method suggested by Warszynski [32] to estimate the work of adhesion when either the tip or the SAM on substrate or both have hydration layers firmly attached to it. By assuming that the dispersion component of the hydrated SAM is the same as that of water and acid-base components of the free energy are equal, we use the measured value of work of adhesion (from AFM pull off force measurements using functionalized tips, where the substrate SAM and the tip have the same function) to estimate the surface energy of the hydration layer. Our estimate matches well with those reported by Warszynski [32]. Knowing this energy we estimate the work of adhesion for the total interaction where either the tip or the substrate or both are hydrated. We obtain a value of work of adhesion, W ($CH_3|H_2O$, $OH|H_2O$, H_2O) = 19.6 mJ/m^2 for the OTS/OH (Si_3N_4) interaction (|denotes hydrated), this compares well with W = 16.5 mJ/m^2 deconvoluted from pull-off force measurement in water medium and is significantly less than the 40.8 mJ/m^2 calculated by considering the SAM as anhydrated. We did similar calculation for FOTS (CF_3 terminal group) and found the work of adhesion (4 mJ/m^2) is close to the experimental W (6.18 mJ/m^2 deconvoluted from pull off force in water) when the FOTS is taken as anhydrated and OH(Si_3N_4) is taken as hydrated. This suggests that for OTS there may be at least a partially water lubricated interface which yields a low F_s while a more unlubricated interface for FOTS gives a higher values of F_s.

We take this argument a little further by recording the LFM images of the two SAMs at this nominal 0% humidity environment. Figure 7 shows that the lateral forces measured within the domains for OTS (10–12 nN) SAM is about the same as that for the FOTS (10–12 nN) SAM but the force measured at the domain boundaries of the FOTS (14–18 nN) is significantly higher than that measured for the OTS (12–13 nN). Pursuing our "hydration" argument presented above we speculate that partial lubrication is achieved in OTS as its domain boundaries attract small amounts of water, perhaps by hydration, to construct a network of lubrication channels. In FOTS the domain boundaries repel water and register regions of high lateral force.

If above is the only effect which controls F_s, a surface further disordered and hydrophilic as in the case of heat-treated SAM should lower the F_s from that recorded in case of non heat-treated SAM. Figure 4 shows that this is clearly not the case. We therefore believe that another independent effect, of conformation disorder which when increased tends to increase channels of energy dissipation [14,15,33,34] and thereby friction, also operates at the terminal end and this opposes the hydration effect which lowers the friction. The overall effect is for the F_s to rise with heat-treatment, which increases conformational disorder. It is possible that for OTS the rise in the F_s is less than that for FOTS because the contact for OTS/OH interaction is at least partially hydrated while for the FOTS it is not.

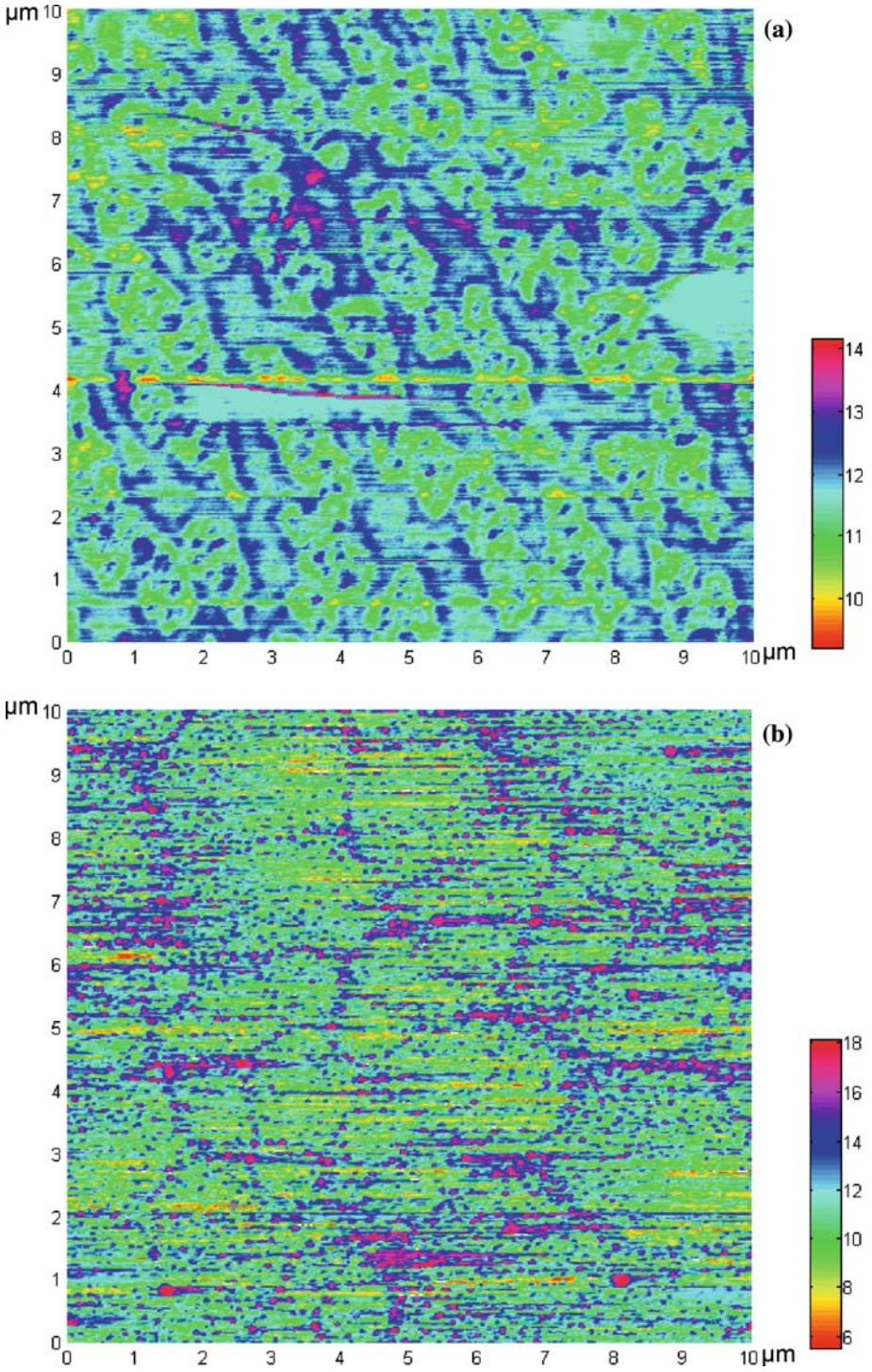

Figure 7. Lateral force images of (a) OTS and (b) FOTS monolayers assembled on mica, taken by atomic force measurements at 0% relative humidity, 0 nN load.

Moving now to $\mu_{k,}$ we observe in figure 4 the following identities in μ_k.

$$\mu_{k(HT)} > \mu_{k(RT)} \text{ and } \mu_{k(FOTS)} > \mu_{k(OTS)}$$

The first identity is perhaps served by the conformational disorder argument but the second is not, as OTS is more disordered than FOTS. We argue that the second identity is caused by the fact that FOTS is a much stiffer molecule than the OTS. This is clearly shown in figure 6 where the contact stiffness data is obtained from measurements using the CFA [26–28]. The FOTS molecule which has a helical backbone structure offers greater lateral resistance to the slider in a collective bending mode than what is done by the OTS

SAM. It should be noted here that heat-treatment of molecules were found to have minimal effect on stiffness. This leads us to conclude that for a given molecule enhancement of friction with heat-treatment is primarily due to an increase brought about thereby in conformational disorder.

Summarizing the LFM results we observe that under these loading conditions despite the fact that the effects are localized in nature, there emerges an overall structure—friction relationship. The interfacial energy and dissipation (F_s) is the resultant of chemical changes such as hydration and opposing physical changes brought about by heat-treatment at the terminal end. The non zero load friction on the other hand is the resultant of two effects; molecular stiffness and conformational disorder both of which raise friction. The stiffness appears to have an important effect as we observe a disordered OTS possessing a weak backbone to register lower friction than FOTS, which is ordered but possesses a stiff backbone. For a given molecule however an increase in disorder is primarily responsible for an increase in friction due to heat-treatment.

We now move to much larger (mN) normal load level experiments in the ambient environment using a nanotribometer. These experiments were very repeatable with hardly any scatter in the results (figure 8). Under this loading (say 50 mN) condition the Hertzian deflection of the SAM (1–2 GPa, Youngs modulus) as an elastic half space is 1–2 μm (this clearly is not possible for a 1.65 nm and 2.5 nm long FOTS and OTS molecules respectively) and that of the aluminium substrate as an elastic half space is about 53 nm. Further the substrate is definitely likely to yield creating a conformal contact. We take the model suggested by Caprick et al. (figure 21, Ref. [12]) where blunt tips trap SAM molecules beyond the plastic limit of the substrate, to describe the contact conditions here. The contact area under these conditions, governed by the modulus and yield stress of the substrate, increase with normal load recovering the Amontons law as seen in figure 8. We are not sure of the actual status of the molecule in this type of contact. Caprick *et al*. [12] suggests that the molecules remain rigid and mildly deformed. Our contact area calculations from the CFA results on the other hand suggest that they are somewhat flattened. In both cases as the slider moves it confronts undeformed molecules, the order/disordered status of which governs the lateral resistance and therefore kinetic coefficient of friction. Figure 8(a) and 8(b) for OTS and FOTS respectively shows that all friction forces unlike in the case of LFM experiments converge to zero at zero normal load. This is most probably because F_s (adhesion force is independent of load and scales with the probe radius; the adhesion force here will be of the order of 10^{-4}N which is within the instrument resolution) falls within instrument resolution and is not measurable. What is interesting is that if we ignore one data point (figure 8(c)) for OTS heat-treated to 483K, (μ_k here is 0.34, a value which approaches a $\mu_k = 0.4$ recorded for the base substrate, this indicates some desorption of SAM at 483 K) the μ_k identities (μ_k; $(FOTS)_{HT} > (FOTS)_{RT} > (OTS)_{HT} > (OTS)_{RT}$), observed in the LFM experiments are reproduced but μ_k is enhanced significantly for the OTS SAM and less pronouncedly for the FOTS SAM over that observed in LFM experiment (figure 4) at normal loads which are six orders different. This enhancement may be due to the fact that the probe in nanotribometry experiment is made of steel. Alternatively or additionally under a more severe (six orders) loading than in LFM experiments more gauche defects are generated [13], this increases the μ_k, the more so for disordered OTS than for the more ordered FOTS. This similarity between the LFM data at 0% RH and nanotribometry data collected in the ambient is indeed remarkable and suggests that the arguments invoked to explain the nN level (μ_k) data may still hold at loads which are six orders higher (the mean pressure of course as noted earlier is not increased but decreases somewhat when the load is increased).

To extend the above arguments further we disperse FOTS and OTS molecules in *n*-hexadecane and use them as lubricants to run a test where an aluminium disc slides against a flat steel pin. We run this test for twenty minutes and record steady state friction coefficient. The results (figure 9) show that the lubricant containing FOTS as well as that containing OTS registers about the same steady state coefficient of friction as yielded by the non heat-treated SAMs in nanotribometry (we do note here that the nanotribometry test and the pin-on-disc tests have both been done using steel probes).

4. Summary

In studying friction of self-assembled monolayers over a six order range of contact radius we find that both molecular stiffness and conformational disorders are major factors which set molecules apart in their frictional responses. A molecule with conformational disorder at the terminal end may develop a hydration layer, the presence of which lowers the level of friction at zero load compared to that of a molecule which has an ordered crystalline structure which renders the molecule hydrophobic. We have found this effect to be pronounced when the contact contains only a few molecules. At this length scale conformational disorder also increases the zero load friction but the increase is seriously modulated by the possibility of hydration of the SAM.

Over the entire range of test length scale and normal load heat treatment of molecules is found to increase coefficient of friction. We believe that this is due to the fact that the enhanced molecular disorder due to heat treatment increases channels of energy dissipation, as

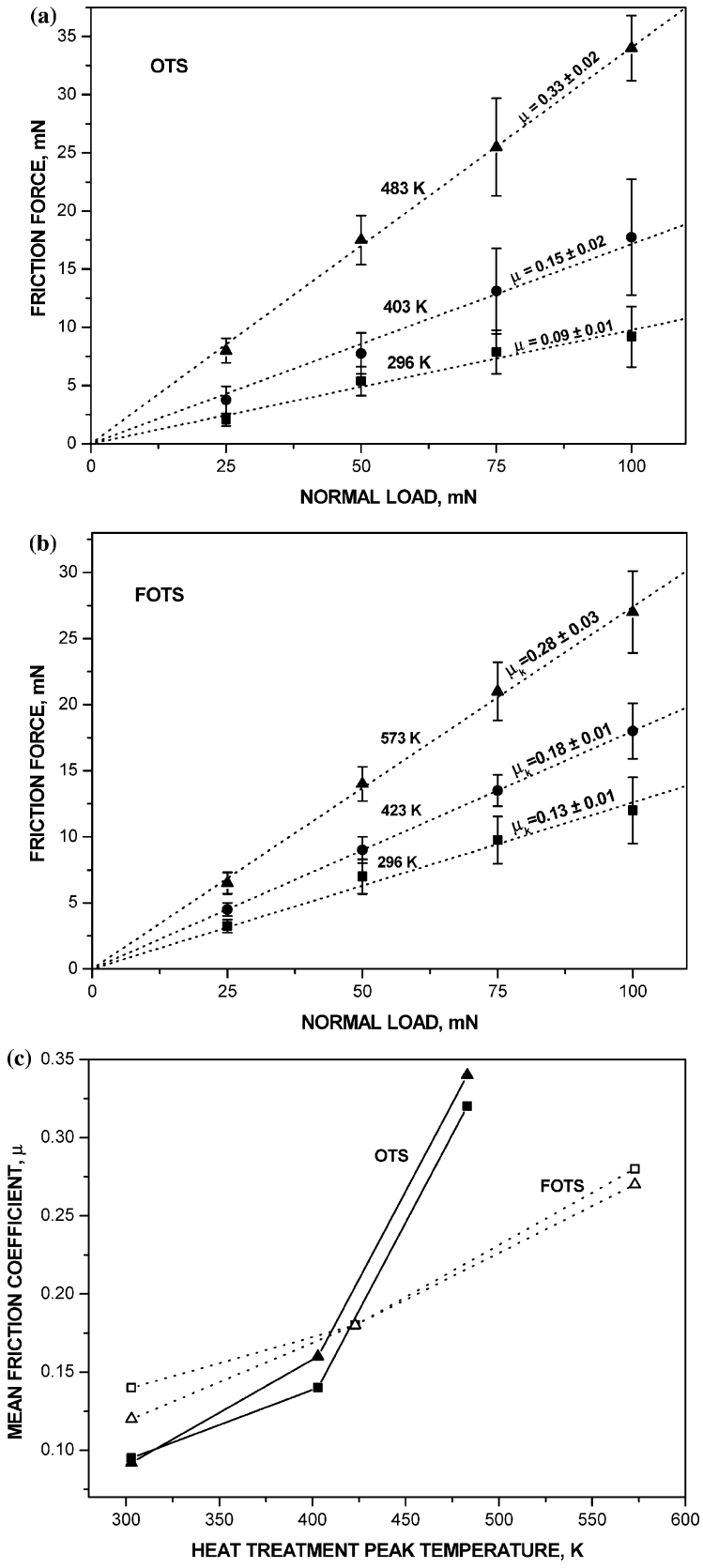

Figure 8. Friction forces measured by nanotribometer at different normal loads for (a) OTS SAM on aluminium against steel ball at different heat-treatment peak temperatures (■) 296 K, (●) 403 K and (▲) 483 K. (b) FOTS SAM at heat-treated peak temperatures (■) 296 K, (●) 423 K and (▲) 573 K (c) Comparison of mean friction coefficient of OTS and FOTS SAM at different peak temperature at two different loads. (■) 50 mN and (▲) 100 mN. Speed: 0.1 cm/sec. Filled symbol is for OTS and open symbol is for FOTS SAM.

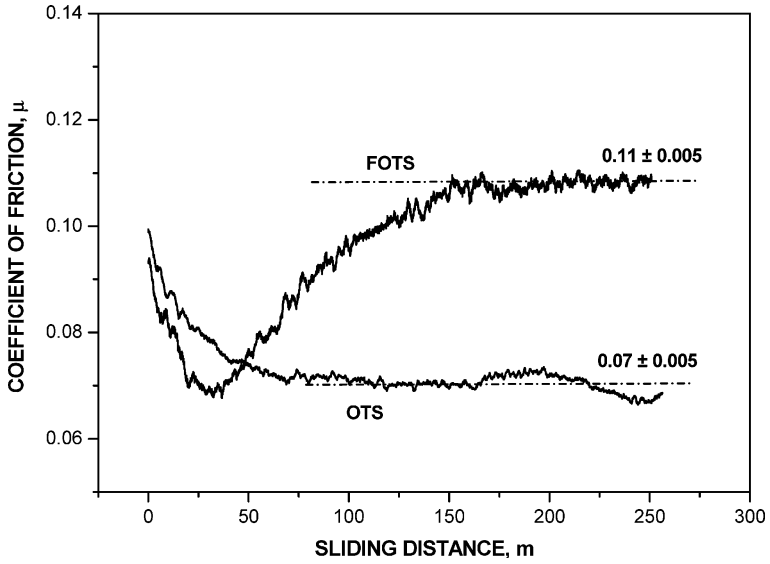

Figure 9. Friction coefficient of steel pin sliding against aluminium disc under lubricated conditions where one drop of lubricant is added to the contact interface at the commencement of experiment. OTS and FOTS additives (5% solution) are dispersed in *n*-hexadecane oil. The friction is recorded in a macrotribometer (pin-on-disc machine). Load: 60 N, speed: 0.2 m/s.

has been noted by earlier workers. If two molecules are however strongly distinguished by molecular stiffness, as one would expect from different back bone conformations, a molecular stiffness, effect overrides the (terminal end) conformational disorder effect. Higher molecular stiffness yields high friction irrespective of the state of order at the terminal end. For a molecule, which has a good crystalline order, it is remarkable to observe that the frictional responses, when the additive is dispersed in oil and that when the molecules are self-assembled on a substrate and tested, are very similar.

Acknowledgments

The authors are grateful to Centre for High Technology (CHT), Ministry of Petroleum, Govt. of India and General Motors (R & D), Warren, USA for the financial grant which has made this work possible. They also acknowledge the help of Ms. N. Prathima, and Mr. H.S. Shamasunder for carrying out this work.

Appendix

Assuming that the contact commences at a distance of σ_s (standard deviation of the effective asperity summit heights) from the mean roughness line we determine penetration δ and contact area A as a function of applied load (see figure 10 A1). For details of estimation of Youngs modulus see Ref. [28]. We first determine the work of adhesion, W between the probe and the monolayer experimentally [24] using contact angle measurement and find for FOTS W≈22 mJ/m^2. We are now in a position to determine an adhesion parameter [28],

$$\theta = \frac{\mathrm{E}^* R^{1/2} \sigma_s^{3/2}}{WR}$$

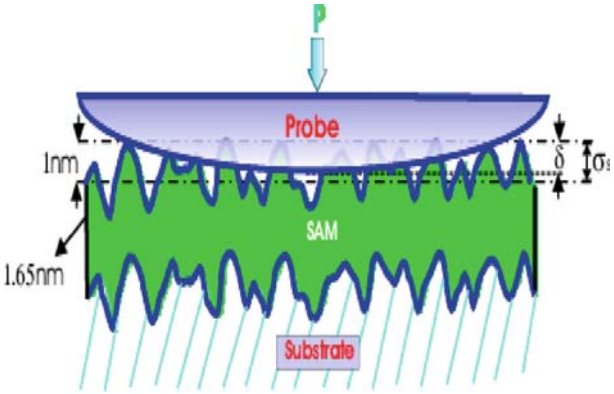

Figure 10 A1. Schematic of contact in a contact force apparatus. σ_s is the effective asperity summit height standard deviation and δ is the penetration. It is assumed that the SAM surface mimics the roughness of the sum roughness of the probe and the substrate.

where

$$\frac{1}{\mathrm{E}^*} = \frac{1 - v_{SAM}^2}{\mathrm{E}_{SAM}} + \frac{1 - v_{\mathrm{Probe}}^2}{\mathrm{E}_{\mathrm{Probe}}}, \mathrm{R} \text{ is the probe radius}$$

The applied load P and real contact area A are;

$$\mathrm{P} = \frac{4}{3} F_{3/2}(d^*) - \frac{2\pi}{\theta} F_{\circ}(d^*) \qquad \text{(A1)}$$

$$A = \pi F_1(d^*) \qquad \text{(A2)}$$

where

$$d^* = \frac{\delta}{\sigma_s},$$

δ is penetration

and $$F_n(d^*) = \frac{1}{\sqrt{2\pi}} \int_{d^*}^{\alpha} (x - d^*)^n \exp\left(-\frac{x^2}{2}\right) dx$$

We solve equation (A1) to obtain penetration for a given applied load and determine real contact area using equation (A2).

References

[1] I.H. Sung, J.C. Yang, D.E. Kim and B.S. Shin, Wear 255 (2003) 808.
[2] A. Takahara, K. Kojio and T. Kajiyama, Ultramicroscopy 91 (2002) 203.
[3] K. Hayashi, H. Sugimura and O. Takai, Appl. Surf. Sci. 188 (2002) 513.
[4] K. Hayashi, H. Sugimura and O. Takai, Jpn. J. Appl. Phys. 40 (2001) 4344.
[5] K. Kojio, A. Takahara and T. Kajiyama, Langmuir 16 (2000) 9314.
[6] S.C. Clear and P.F. Nealey, J. Colloid. Interface Sci. 213 (1999) 238.
[7] D. Devaprakasam, S. Sampath and S.K. Biswas, Langmuir 20 (2004) 1329.
[8] O.P. Khatri and S.K. Biswas, Surf. Sci. 572 (2004) 228.
[9] N.A. Burnham, D.D. Dominguez, R.L. Mowery and R.J. Colton, Phys. Rev. Lett. 64 (1990) 1931.
[10] A. Lio, D.H. Charych and M. Salmeron, J. Phys. Chem. B 101 (1997) 3800.
[11] M. Graupe, T. Koini, H.I. Kim, N. Garg, Y.F. Miura, M. Takenaga, S.S. Perry and T.R. Lee, Colloids Surfaces A. 154 (1999) 239.
[12] R.W. Carpick and M. Salmeron, Chem. Rev. 97 (1997) 1163.
[13] P.T. Milkulski and J.A. Harrsion, J. Am. Chem. Soc. 123 (2001) 6873.
[14] X. Yang and S.S. Perry, Langmuir 19 (2003) 6135.
[15] M.T. McDermott, J.D. Green and M.D. Porter, Langmuir 13 (1997) 2504.
[16] M. Granier, G.F. Lanneau, J. Moineau, P. Girard and M. Ramonda, Langmuir 19 (2003) 2691.
[17] W. Lu and Z. Suo, Phys. Rev. B 65 (2002) 205418.
[18] A. Noy, S. Zepeda, C.A. Orme, Y. Yeh and J.J.D. Yoreo, J. Am. Chem. Soc. 125 (2003) 1356.
[19] J.I. Siepmann and I.R. McDonald, Phys. Rev. Lett. 70 (1993) 453.
[20] E. Barrena, C. Ocal and M. Salmeron, J. Chem. Phys. 113 (2000) 2413.
[21] A.B. Tutein, S.J. Stuart and J.A. Harrison, Langmuir 16 (2000) 291.
[22] P.C. Nalam, M. Harini, R. Neeraj, R.H. Chadrashekara, K.G. Ayappa, S. Sampath and S.K. Biswas, Langmuir 21 (2005) 2364.
[23] H.I. Kim, T. Koini, T.R. Lee and S.S. Perry, Langmuir 13 (1997) 7192.
[24] D.K. Owens and R.C. Werdt, J. Appl. Pol. Sci. 13 (1969) 1741.
[25] D. Devaprakasam, O.P. Khatri, N. Shankar and S.K. Biswas, Tribol. Intl. (In-press).
[26] D. Devaprakasam and S.K. Biswas, Rev. Sci. Instrum. 74 (2003) 1228.
[27] D. Devaprakasam and S.K. Biswas, Rev. Sci. Instrum. 76 (2005) 0351021–7.
[28] D. Devaprakasam and S.K. Biswas, Phys. Rev. B 78 (2005) 125434.
[29] L. Qian, F. Tian and X. Xiao, Tribo. Lett. 15 (2003) 169.
[30] X. Xiao and L. Qian, Langmuir 16 (2000) 8153.
[31] M. He, A.S. Blum, D.E. Aston, C. Buenviaje and R. Luginbuhl, J. Chem. Phys. 114 (2001) 1355.
[32] P. Warszynski, G. Papastavrou, K.D. Wantke and H. Mohwald, Colloids Surfaces A 214 (2003) 61.
[33] H. Schonherr and G.J. Vancso, Mater. Sci. Eng. C 8–9 (1999) 243.
[34] X. Xiao, J. Hu, D.H. Charych and M. Salmeron, Langmuir 12 (1996) 235.